ACADEMIC PRESS

Available online at www.sciencedirect.com

SCIENCE DIRECT®

VIROLOGY

Virology 317 (2003) 50–64

www.elsevier.com/locate/yviro

The conserved structures of the 5′ nontranslated region of *Citrus tristeza virus* are involved in replication and virion assembly

Siddarame Gowda,[a] Tatineni Satyanarayana,[a] María A. Ayllón,[a] Pedro Moreno,[b] Ricardo Flores,[c] and William O. Dawson[a,*]

[a] *Department of Plant Pathology, University of Florida, Citrus Research and Education Center, Lake Alfred, FL 33850, USA*
[b] *Instituto Valenciano de Investigaciones Agrarias, 46113, Moncada, Valencia, Spain*
[c] *Instituto de Biología Molecular y Cellular de Plantas, Universidad Politécnica de Valencia, Valencia, Spain*

Received 30 June 2003; returned to author for revision 6 August 2003; accepted 19 August 2003

Abstract

The genomic RNA of different isolates of *Citrus tristeza virus* (CTV) reveals an unusual pattern of sequence diversity: the 3′ halves are highly conserved (homology >90%), while the 5′ halves show much more dissimilarity, with the 5′ nontranslated region (NTR) containing the highest diversity (homology as low as 42%). Yet, positive-sense sequences of the 5′ NTR were predicted to fold into nearly identical structures consisting of two stem-loops (SL1 and SL2) separated by a short spacer region. The predicted most stable secondary structures of the negative-sense sequences were more variable. We introduced mutations into the 5′ NTR of a CTV replicon to alter the sequence and/or the predicted secondary structures with or without additional compensatory changes designed to restore predicted secondary structures, and examined their effect on replication in transfected protoplasts. The results suggested that the predicted secondary structures of the 5′ NTR were more important for replication than the primary structure. Most mutations that were predicted to disrupt the secondary structures fail to replicate, while compensatory mutations were allowed replication to resume. The 5′ NTR mutations that were tolerated by the CTV replicon were examined in the full-length virus for effects on replication and production of the multiple subgenomic RNAs. Additionally, the ability of these mutants to produce virions was monitored by electron microscopy and by passaging the progeny nucleocapsids to another batch of protoplasts. Some of the mutants with compensatory sequence alterations predicted to rebuild similar secondary structures allowed replication at near wild-type levels but failed to passage, suggesting that the 5′ NTR contains sequences required for both replication and virion assembly.

Keywords: CTV; Closterovirus; 5′ Nontranslated region

Introduction

Citrus tristeza virus (CTV) of the genus *Closterovirus* is a monopartite member of the *Closteroviridae*. The ~20-kb single-stranded plus-sense RNA genome is organized into 12 open reading frames (ORFs) (Pappu et al., 1994; Karasev et al., 1995). The 5′ proximal ORF 1a encodes a 349-kDa protein containing two papain-like protease domains, plus methyltransferase-like and helicase-like domains; occasionally, translation continues, presumably by a +1 frameshift into ORF 1b producing an RNA-dependent RNA polymerase domain (Karasev et al., 1995). The 3′ half of the genome contains 10 ORFs that are expressed via 3′-coterminal sgRNAs (Hilf et al., 1995).

In addition to having sequences encoding proteins for the viral life cycle, RNA viruses contain regulatory *cis*-acting elements that are involved in a range of functions, including initiation of minus-stranded RNAs and subgenomic RNAs (sgRNAs), initiation of virion assembly, regulation of gene expression, and probably movement within the host and induction of diseases (reviewed by Duggal et al., 1994; Buck, 1996; Miller et al., 1998; Turner and Buck, 1999; Miller and Koev, 2000). *Cis*-acting elements within the 3′

* Corresponding author. University of Florida, Citrus Research and Education Center, 700 Experiment Station Road, Lake Alfred, FL 33850.
E-mail address: wodtmv@lal.ufl.edu (W.O. Dawson).

0042-6822/$ – see front matter © 2003 Elsevier Inc. All rights reserved.
doi:10.1016/j.virol.2003.08.018

nontranslated region (NTR) that serve as promoters for minus-strand synthesis have been extensively characterized, with both primary and secondary structures required (Dreher, 1999). Although 5′ NTR sequences also are required for replication, there is less information concerning their specific function. By analogy to the *cis*-acting elements in the 3′ NTR, structures in the 3′ terminus of the minus-strand (complement to the 5′ NTR) might be expected to function as the plus-strand promoter (Guan et al., 1997; Sivakumaran and Kao, 1999; Nagy and Pogany, 2000; Panavas and Nagy, 2003; Panavas et al., 2003). Yet, in some cases the functional element appears to be in the positive-strand sequence. For example, the 5′ *cis*-acting elements of *Brome mosaic virus* (BMV) that resemble internal control region-like (ICR) motifs of tRNA promoters (Marsh and Hall, 1987) were shown to function in the positive-strand (Pogue and Hall, 1992). Also, sequences in the 5′ NTR have been shown to be involved in the initiation of minus-strand synthesis in poliovirus (Barton et al., 2001) and yellow fever virus (Corver et al., 2003). Further, both 3′ and 5′ terminal sequences of the minus-strand template were demonstrated to be required for the plus-strand RNA synthesis of satRNA C templates of *Turnip crinkle virus* (TCV) in vitro (Guan et al., 1997). Additionally, origins of assembly of RNA viruses can reside in the 5′ NTR as has been shown for Potexviruses (Abouhaidar and Bancroft, 1978; Sit et al., 1994). Thus, even when RNA viruses are found to have regulatory elements associated with the 5′ end of the genomic RNAs, there is no clear expectation in which strand (plus or minus) the *cis*-acting element is active or for what function.

Sequences of different strains of CTV reveal unusual sequence diversity (Mawassi et al., 1996; Albiach-Marti et al., 2000). Although the 3′ portions (approximately half) of all genomes vary by about 10% or less, the 5′ portions of the genomes differ dramatically, much more than expected for strains of the same virus. The level of sequence diversity peaks near the 5′ terminus, with sequence similarities as low as 40%. López et al. (1998) analyzed the terminal sequences of 10 isolates of CTV representing three groups that differ by up to 56% in the 5′ NTR, yet found that all were predicted to fold into almost identical structures consisting of two stem-loops (SL). The remarkable conservation of the predicted structures amid such variation in sequence suggested that the putative structures were likely both real and functional.

We previously examined the compatibility of heterologous CTV 5′ NTRs with the replicase complex by substitution of 5′ terminal regions from other strains into a CTV replicon containing large internal deletion (Satyanarayana et al., 1999). The replication continued moderately with 5′ NTRs from strains with more similar sequences, but replication was substantially reduced with 5′ NTRs from strains of more distantly related biological groups (Satyanarayana et al., 1999). Substitution of 5′ segments much larger than the 5′ NTR (up to 1000 nucleotides; nts) decreased replication no more than the exchange of only the 5′ NTR (Satyanarayana et al., 1999), suggesting that most of the necessary *cis*-acting elements required for replication were contained within the 5′ NTR.

Here we report the analysis of the predicted structures within the 5′ NTR relative to replication and assembly of CTV. Mutations that altered the predicted structures prevented replication. However, most mutations that were designed to alter the sequence, but with compensatory changes predicted to restore secondary structures, resulted in continued replication, suggesting that the secondary structures of the 5′ NTR were important for replication of CTV. Yet, several mutants with altered sequences but compensatory changes to maintain the predicted secondary structures and near wild-type levels of replication in *Nicotiana benthamiana* protoplasts failed to be passaged to the next set of protoplasts, suggesting that the 5′ NTR contains elements required for virion assembly.

Results

Examination of predicted folding patterns of the 5′ NTR of CTV isolates

Both positive- and negative-sense sequences of the 5′ NTR of CTV T36 isolate, consisting of 107 nts (Fig. 1A), were analyzed with the *MFOLD* program of Zuker et al. (1999) to predict secondary structures. The sequence of the positive-sense 5′ NTR was predicted to fold at 37°C into two stem-and-loop structures with a short intervening single-stranded spacer region and single-stranded 5′ (nts 1 to 16) and 3′ (nts 90 to 107) regions with a free energy of −22.01 kcal/mol (Fig. 1B). We refer to the predicted secondary structures as stem-loop 1 (SL1: nts 17 to 51) and stem-loop 2 (SL2: nts 57 to 89) separated by a spacer sequence (nts 52 to 56). The *MFOLD* program predicted a slightly less-stable alternative structure (dG = −21.31 kcal/mol) with identical SL1, spacer, and SL2 structures, but with an additional short stem formed by base pairing of a portion of the single-stranded 5′ and 3′ regions (nts 1 to 5 with nts 98 to 102) (Fig. 1C). Further, the 5′ NTR yielded a similar predicted secondary structure at folding temperatures ranging between 22 and 55°C (data not shown), and the conservation of SL1 and SL2 regions was observed when 250 nts of the 5′ terminal region were analyzed (Fig. 1F; positions of SL1 and SL2 have been highlighted), suggesting that the predicted SL structures of the 5′ NTR of the positive-sense sequence represent stable structures.

New sequences of CTV isolates that fall into different biological groups (strains) are now available in addition to those examined by López et al. (1998). We analyzed representatives of these groups to determine whether all 5′ NTR sequences fold into similar structures. The lengths of the 5′ NTRs vary: T68, 102 nts; VT, NuagA, and SY568, 105 nts; T36 and T30, 107 nts; T385, 108 nts; T3, 109 nts

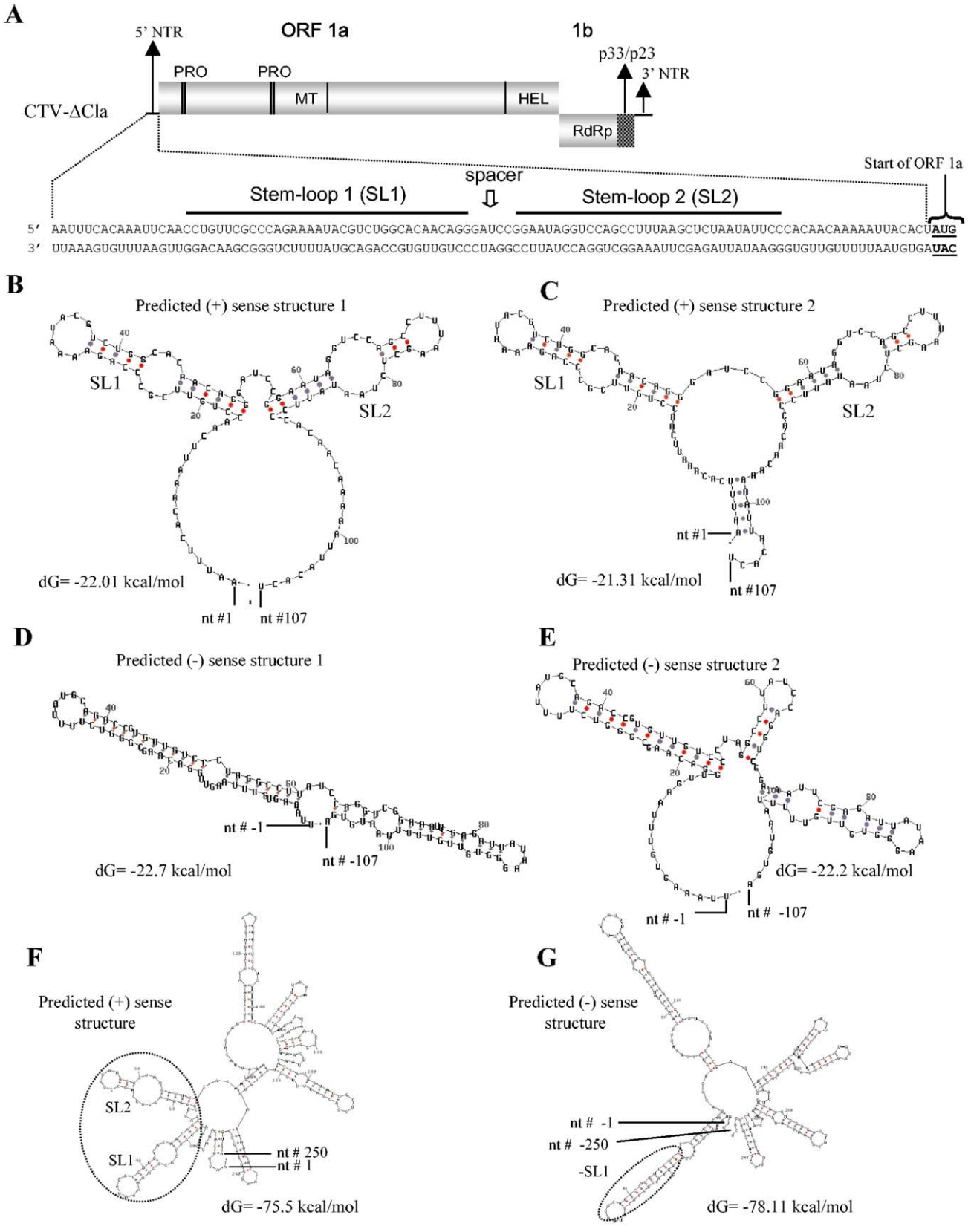

Fig. 1. (A) Schematic representation of the CTV T36 replicon, CTV-ΔCla (Satyanarayana et al., 1999). The open boxes represent the open reading frames (ORFs). CTV-ΔCla contains ORF 1a and 1b and a chimeric region toward the 3′ end formed by the fusion of the 5′ proximal end of ORF 2 that encodes the putative p33 protein and the distal portion of the 3′ most ORF, ORF11, that encodes p23 protein. A 107-nt 5′ nontranslated region (NTR) at the 5′ end and a 273-nt 3′ NTR at the 3′ end are also indicated. The nucleotide sequence of the 5′ NTR and the positions of the predicted stem-loop (SL) regions 1 and 2 and the spacer region between the SL regions are also shown. The predicted secondary structures using the *MFOLD* program (Zuker et al., 1999) of the 5′ NTR in the positive sense (B and C), the negative sense (D and E), and the major type of predicted structure of the 5′ proximal 250-nt region in the positive-(F) and negative-(G) sense, and their respective free energies, are also indicated. The positions of the first and the last nucleotides and the predicted positions of the SL1 and SL2 in secondary structures are also indicated.

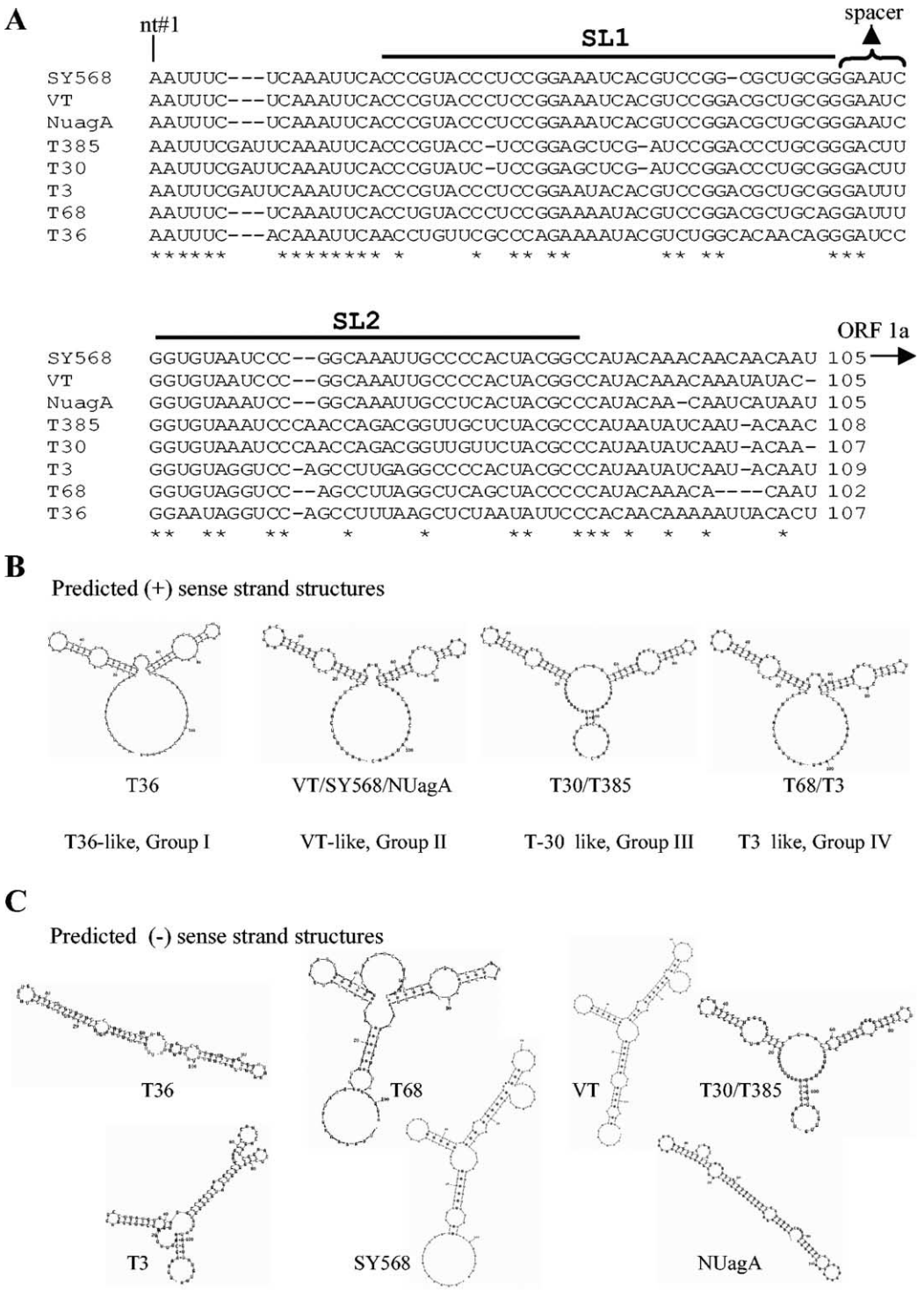

Fig. 2. (A) Multiple alignment of the 5′ NTRs of various isolates of CTV that belong to different biological groups using the CLUSTAL program. The GenBank Accession Nos. of the CTV isolates used for analysis are as follows: SY568, AF001623; VT, U56902; NuagA, AB046398; T385, Y18420; T30, AF260651; T36, NC_001661; T3 and T68 (M. Hilf, personal communication). The asterisks represent the nucleotides conserved in all the isolates. The number of nucleotides in the 5′ NTR of various CTV isolates is indicated at the right of the sequence. The predicted positions of the SL1 and SL2 and the spacer region are shown by dark lines and a bracket, respectively, above the sequence. The predicted secondary structures of the plus-(B) and minus-strand (C) of the 5′ NTR of different isolates of CTV are also shown.

(Fig. 2A). The 5′ terminal nucleotide of all isolates was an adenylate (A), and all contained conserved stretches of 6 nts (AAUUUC, nts 1 to 6) and 8 nts (CAAAUUCA; nts 8 to 15 in T36) (Fig. 2A). Otherwise, the 5′ NTRs represent the most highly variable region in the CTV genome, as low as 42% homology between the two Florida isolates T36 and

T30 (Albiach-Martí et al., 2000). The predicted secondary structure of the 5′ NTRs of T3, T68, NUagA, VT, and SY568 were similar to the predicted structure 1 of T36 (Figs. 1B and 2B), while T30 and T385 were predicted to fold into structures similar to the predicted structure 2 of T36 (Figs. 1C and 2B). Thus, despite the sequence variation, the positive-sense sequence of all CTV 5′ NTRs from the different biological groups were predicted to fold into similar SL1 and SL2 structures, separated by a small single-stranded spacer.

We next analyzed the complementary sequences. For simplicity, we used positive-strand numbering with a negative sign preceding the nucleotide number. Thus, the 3′ terminal nucleotide (in the minus strand), complementary to nt 1 (of the positive strand), was labeled nt −1. The sequence complementary to the 5′ NTR of T36 was predicted to fold into two different structures with free energies of −22.7 and −22.2 kcal/mol (Figs. 1D and E). Neither predicted negative-strand structure was the mirror image of either of the predicted positive-strand structures. The predicted negative-sense secondary structure of the first stem loop was conserved when 250 nts of the 5′ terminus were analyzed, but other predicted structures were not (Fig. 1G; the position of the first stem loop is highlighted). When the negative-sense sequences of other CTV groups were analyzed, ranges of dissimilar structures were predicted (Fig. 2C). Thus, the predicted secondary structures of the plus-strand sequences were conserved among different groups, whereas those predicted for the minus-strand sequences appeared not to be conserved.

Mutational analysis of the 5′ NTR

To examine whether the predicted secondary structures of the 5′ NTR of CTV T36 were involved in virus replication, mutations were introduced into CTV-ΔCla, a CTV replicon with all of the 3′ genes deleted (Satyanarayana et al., 1999), and accumulation of the genomic RNA and the p33/p23 chimeric sgRNA was determined after infection of mesophyll protoplasts of *N. benthamiana*. Because the structures predicted from the positive-sense 5′ NTRs appeared to be more conserved among the different groups, we used the common predicted structure 1 with positive-strand numbering as a model. Mutations included those that were designed to alter the predicted secondary structures and compensatory changes predicted to restore the original structures plus deletions and/or substitutions with nonviral sequences into the loop and spacer regions. These experiments allow discrimination between mutations that allow viral RNA accumulation and those that prevent RNA accumulation, but since detectable CTV RNA replication in protoplasts requires amplification by unknown rounds of replication, it is not possible to define the specific steps that prevented replication. The results presented were repeated independently four to five times with two to three independent clones of each mutant.

Changes in the 5′ and 3′ proximal regions of the 5′ NTR

Nucleotides 1 to 16 and 90 to 107 are predicted to be single stranded by *MFOLD* in most sequence groups, but occasionally were predicted to fold into a short double-stranded structure [T36 (structure 2), VT (not shown), T30, and T385] (Figs. 1C and 2B). Mutants CTV-ΔCla M1 and CTV-)Cla M2 contained deletions of the 5′ terminal 9 and 14 nts, respectively, while mutant CTV-ΔCla M3 contained a substitution of nts 10 to 14 (5′-3′ AAUUC) with nonviral nucleotides (5′-3′ UGCAU) (Fig. 3A). These changes did not alter predicted structure 1 (Fig. 3B). RNA transcripts from these mutants were transfected into *N. benthamiana* protoplasts, and the total RNA samples isolated at 3 and 4 days postinoculation (dpi) were analyzed by Northern hybridization using 3′ plus- or minus-strand-specific riboprobes. Mutant CTV-ΔCla M1 replicated and produced both plus- and minus-stranded genomic and sgRNAs at only slightly reduced levels (Fig. 3C). It is unusual to be able to delete 9 nts from the 5′ terminus of a viral RNA with continued replication, but it should be noted that the context of the 5′ end nucleotides was similar in CTV-ΔCla (5′- 3′ AAUUUCAA) and CTV-ΔCla M1(5′- 3′ AAUUAA). Deletion of the 5′ 14 nts of CTV-ΔCla M2 resulted in a context change in the 5′ terminus and completely abolished replication (Fig. 3C). Yet, mutant CTV-ΔCla M3, which disrupted the nucleotide context that is conserved in all sequences (5′- 3′ CAAAUUCA, nts 8–15) (Fig. 2A) by substitution of nonviral sequences (resulting in 5′- 3′ CAUGCAUA), replicated well, demonstrating that these conserved sequences were not necessary for replication.

Changes also were introduced in the 3′-proximal region (nts 90 to 107) of the 5′ NTR. Mutants CTV-ΔCla M4 and CTV-ΔCla M5 contained deletion of nucleotides 98 to 107 and 92 to 107, respectively (Fig. 3A). These changes were predicted to reduce the length of the 3′-proximal single-stranded region and to abrogate the formation of the small helix between this region and the 5′ nucleotides for some of the groups, but not to alter the predicted structures of SL1 and SL2 (Fig. 3B). Both mutants replicated in protoplasts, yet CTV-ΔCla M4 and CTV-ΔCla M5 accumulated genomic and sgRNAs at reduced levels compared to that of CTV-ΔCla (Fig. 3C). These results demonstrate that the sequences in both the 5′ and the 3′ proximal termini of the 5′ NTR tolerate deletions or mutations.

As indicated, none of the mutations altered the predicted positive-stranded structures (Fig. 3B). The minus-strand secondary structures of mutants CTV-)Cla M1, CTV-)Cla M2, and CTV-ΔCla M3 were predicted to be similar to minus-strand structure 2 of wild-type CTV-ΔCla, but the secondary structures predicted for mutants CTV-ΔCla M4 and CTV-ΔCla M5 were altered, retaining only the SL1 (data not shown).

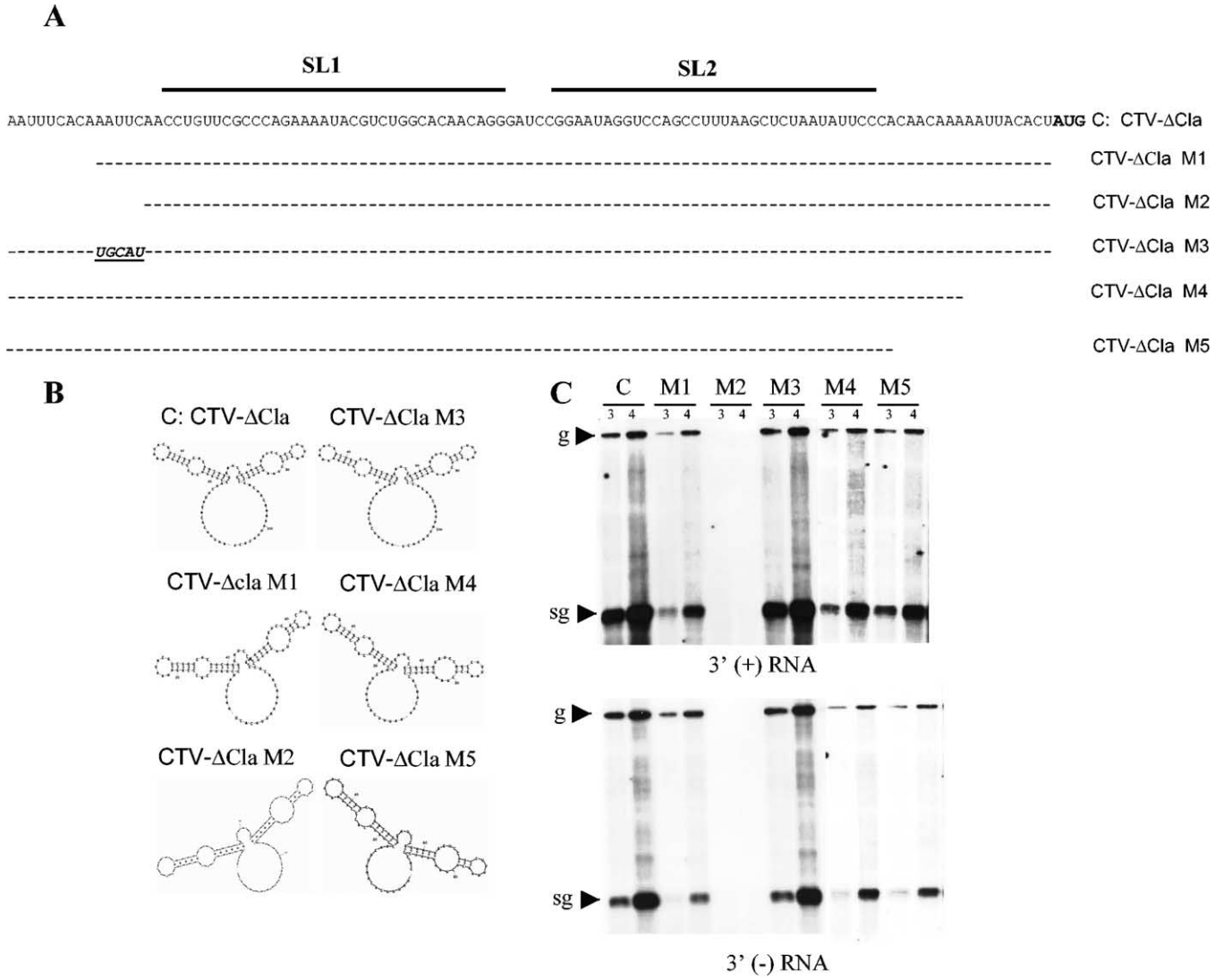

Fig. 3. Mutational analysis of the 5′ and 3′ regions of the 5′ NTR. (A) Schematic representation of the deletions (blank regions) and substitution (in italics and underlined) introduced in the 5′ and 3′ regions of the 5′ NTR. Sequence of the 5′ NTR and the predicted positions of SL1 and SL2 (thick dark lines above the sequence) are indicated. The nucleotides that were not changed are shown by dashes. (B) The predicted secondary structure of the positive-sense 5′ NTR of mutants CTV-ΔClaM1 through CTV-ΔClaM5 and the wild-type 5′ NTR (CTV-ΔCla). (C) Northern blot analysis of the total RNA isolated from 3 and 4 days postinoculated *N. benthamiana* protoplasts with the capped transcripts of the mutants CTV-ΔClaM1 through CTV-ΔClaM5 and the parental CTV-ΔCla. The blots were hybridized with 3′ positive-stranded RNA (top) or negative-stranded RNA (bottom) specific digoxigenin-labeled riboprobes. Positions of the genomic (g) and subgenomic (sg) RNAs are indicated by arrowheads.

Mutations in the spacer region between SL1 and SL2 sequences

A single-stranded spacer region of 5 nts (nts 52 to 56; 5′-3′ GAUCC) was predicted between SL1 and SL2 of the positive-sense 5′ NTR secondary structure of T36. Mutants were created to contain a deletion of the spacer region (CTV-ΔCla M6), a substitution of nucleotides of the spacer region with nonviral nucleotides (CTV-ΔCla M7: 5′-3′ AGCAU), and an insertion of seven nonviral nucleotides to increase the distance between SL1 and SL2 (CTV-)Cla M8: 5′-3′ GA*CAUCGAU*UCC; the additional nucleotides are shown in italics) (Fig. 4A). The predicted secondary structures showed close juxtaposition of SL1 and SL2 for CTV-ΔCla M6 and widely separated SL1 and SL2 for CTV-ΔCla M8, while no change in the basic structure was predicted for CTV-ΔCla M7 (Fig. 4B). Mutants CTV-ΔCla M7 and CTV-ΔCla M8 replicated in protoplasts and accumulated genomic and sgRNAs at approximately similar levels to that of wild-type CTV-ΔCla, while CTV-ΔCla M6 replicated at much reduced levels (Fig. 4C). The presence of a nonviral or a larger spacer region allowed replication at near wild-type levels. Thus, a spatial separation of the SL1 and SL2 sequences appears to be essential for optimal replication, but the sequence of the spacer region probably is not a necessary component of this *cis*-acting element.

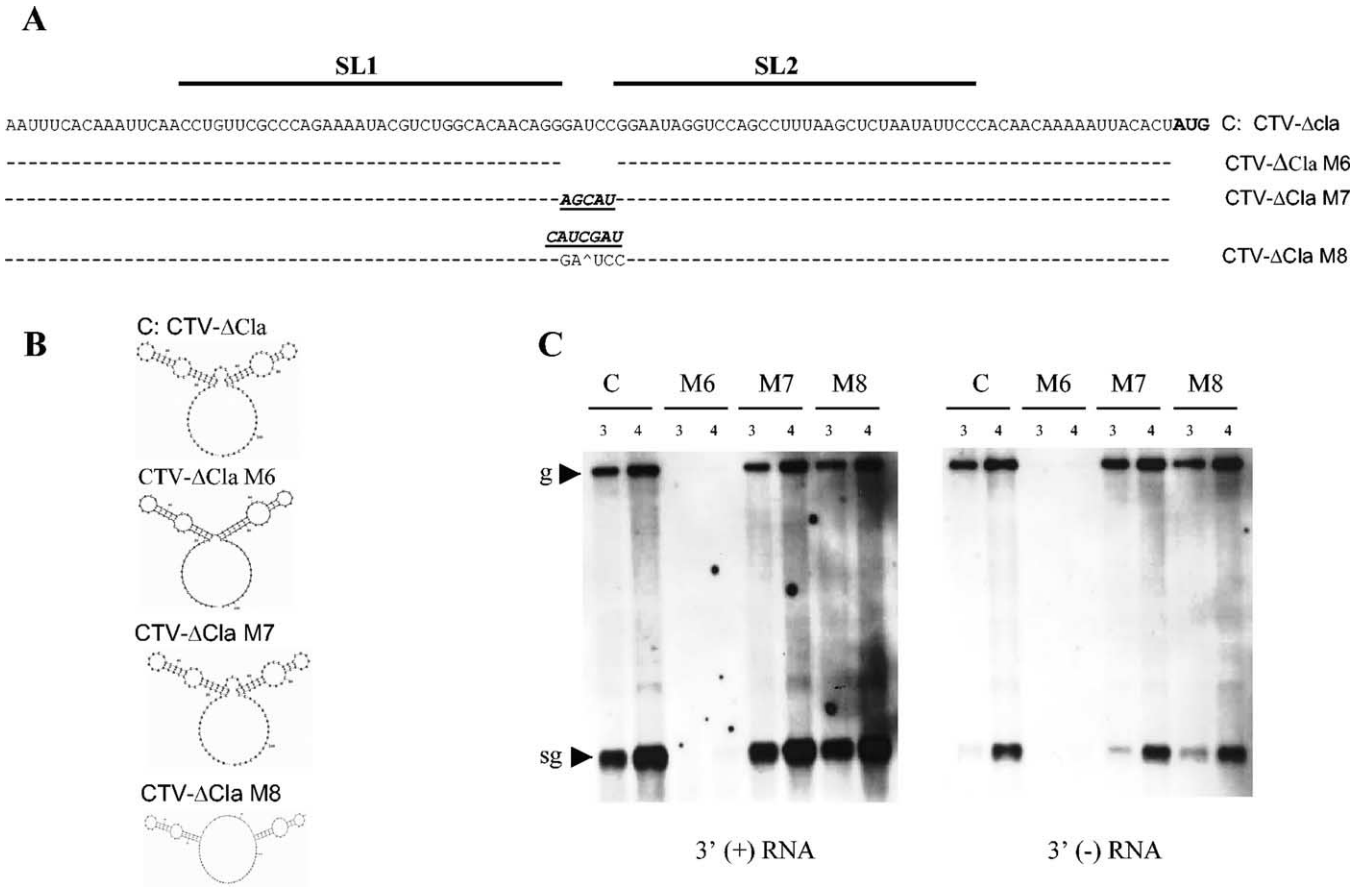

Fig. 4. (A) Schematic representation of the mutations in the spacer region of 5′ NTR. Deletion of the spacer (deleted nucleotides shown by blank region; CTV-ΔClaM6); nonviral spacer (nonviral nucleotides in italics and underlined; CTV-ΔClaM7), and extended spacer (inserted nonviral nucleotides into the spacer region; CTV-ΔClaM8), and the sequence of the parental replicon, CTV-ΔCla are shown. The dashes indicate unchanged nucleotides. (B) The predicted secondary structure of the plus-sense 5′ NTR sequence of wild-type (CTV-ΔCla) and the mutants CTV-ΔClaM6 to CTV-ΔClaM8. (C) Northern blot analysis of the total RNA isolated from the mesophyll protoplasts of *N. benthamiana* at 3 and 4 days after infection with the RNA transcripts from CTV-ΔCla and the mutants CTV-ΔClaM6 to CTV-ΔClaM8. The blots were hybridized with positive-sense RNA-specific (left) or negative-sense RNA-specific (right) digoxigenin-labeled riboprobes. The arrowheads indicate the positions of the genomic (g) and subgenomic (sg) RNAs.

Mutations in SL2

Mutant CTV-ΔCla M9 contained a deletion of 10 nts (nts 69 to 78; 5′-3′ GCCUUUAAGC) that was predicted to constitute the terminal portion of SL2 (Fig. 5A). This deletion was predicted to change the secondary structure of 5′ NTR by the absence of the terminal SL2 region (Fig. 5B). This deletion mutant replicated at levels similar to that of the wild-type CTV-ΔCla, suggesting that the predicted terminal SL2 region had only a minor role in the replication of CTV (Fig. 5C). Mutant CTV-ΔCla M10 contained a substitution of the nucleotides in the left side of the lower stem with nonviral nucleotides (nts 57 to 62; 5′-3′ GGAAUA changed to UAUUCC), and the mutant CTV-ΔCla M11 contained compensatory changes into CTV-ΔCla M10 at nucleotides 84 to 89 (5′-3′ UAUUCC changed to GGAAUA). The mutation of CTV-ΔCla M10 was predicted to completely destroy the structure of SL2, while the compensatory mutation of CTV-ΔCla M11 was predicted to restore the structure similar to that of the wild-type SL2 (Fig. 5B). Mutant CTV-ΔCla M10 replicated at much reduced levels, while the compensatory change with nonviral sequences in mutant CTV-ΔCla M11 restored replication to approximately wild-type levels (Fig. 5C). These results suggest that maintenance of the helical structure at the base of SL2 was essential for replication, but that the primary structure in this area was less important.

Mutations in SL1

Mutants were designed to disrupt the basal and upper stem with nonviral nucleotides and to rebuild the helix with corresponding compensatory changes. We also constructed mutations that deleted the terminal loop region and altered the loop region with nonviral nucleotides. Mutant CTV-ΔCla M12 contained a substitution of nucleotides affecting one chain of the helix of the basal stem of SL1 (nts 17 to 21; 5′-3′ CCUGU changed to AGAUC) (Fig. 6A). This mutation was predicted to result in an altered secondary structure in which both SL1 and SL2 were juxtaposed with no spatial

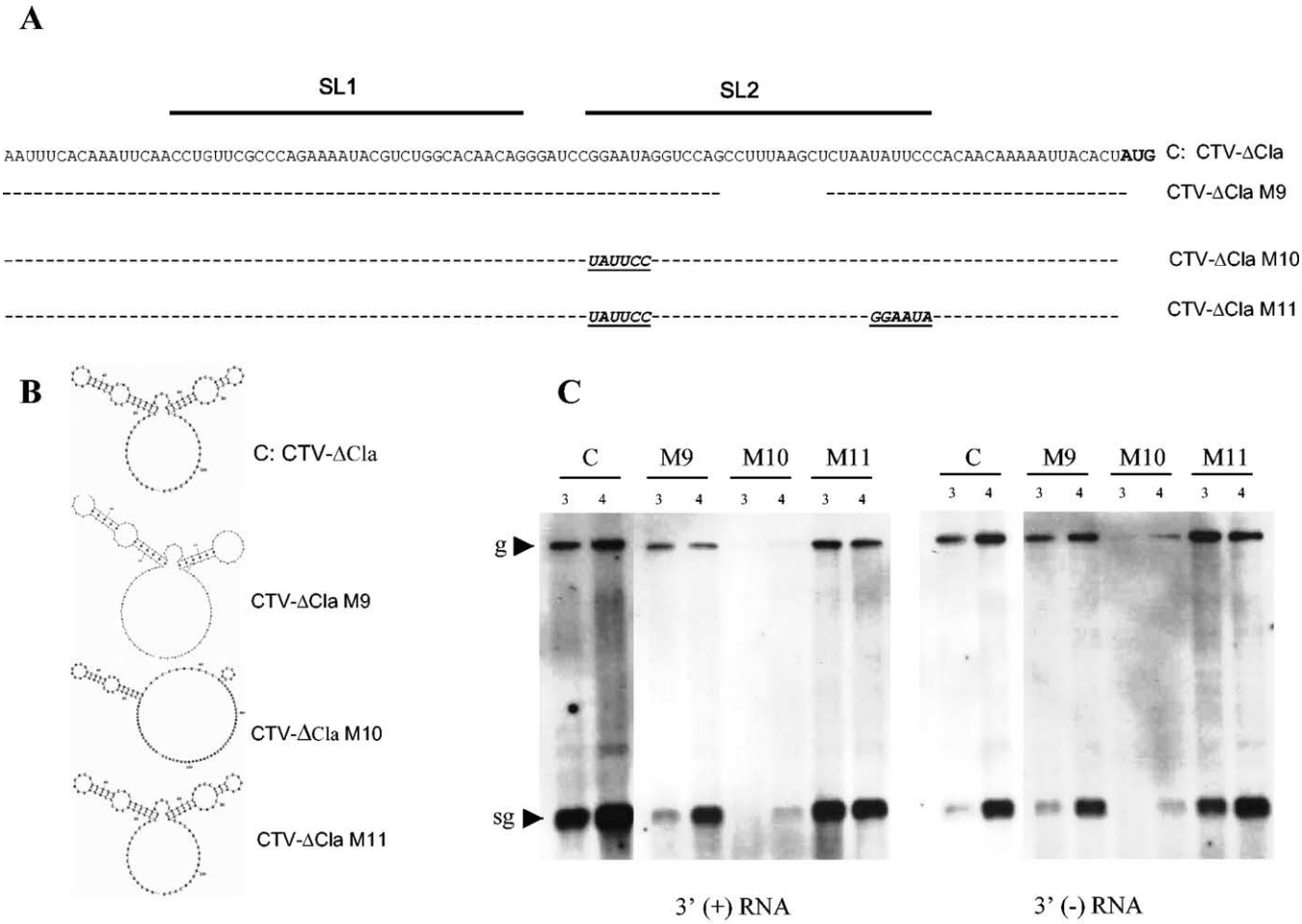

Fig. 5. (A) Mutational analysis of the SL2 of the 5′ NTR. The nucleotide sequence of the wild-type 5′ NTR (CTV-)Cla) is presented and the positions of the predicted SL1 and SL2 are indicated by thick lines above the sequence. The deletion of the nucleotides of the terminal-loop (CTV-)ClaM9), the substitution of the stem with nonviral nucleotides (CTV-)ClaM10), and mutation with compensatory change (CTV-)ClaM11) are shown. (B) The predicted secondary structure of the positive-sense 5′ NTR of wild-type and the mutants are presented. (C) Northern blot analysis of the total RNA isolated from protoplasts 3 and 4 days posttransfection with the RNA transcripts from parental and the 5′ NTR SL2 mutants. The blots were hybridized with positive-sense RNA specific (left) or negative-sense RNA specific (right) digoxigenin-labeled riboprobes. Locations of the genomic (g) and subgenomic (sg) RNAs are shown by arrowheads.

separation (similar to that predicted for mutant M6); the basal loop was enlarged, and the resulting stem was shifted by 5 nts (Fig. 6B). This mutant failed to replicate to detectable levels (Fig. 6C). CTV-ΔCla M13, which contained additional nucleotide changes designed to provide compensatory changes to rebuild the helix of the basal stem region of SL1 (nts 47 to 51; 5′-3′ ACAGG changed to GAUCU in mutant CTV-ΔCla M12) (Fig. 6B), accumulated slightly reduced levels of genomic and sgRNA compared to the wild-type construct (Fig. 6C). Similarly, mutants CTV-)Cla M14 (nts 26 to 29; 5′-3′ CCAG changed to UAGC) and CTV-ΔCla M15 (nts 39 to 42; 5′-3′ CUGG changed to GCUA in mutant CTV-ΔCla M14) were designed to disrupt and rebuild the top helix of SL1, respectively. CTV-ΔCla M14, which was predicted to retain the upper stem of SL1, increased the length of the stem by one nucleotide pair, reduced the size of the internal loop, and failed to replicate; while its compensatory mutant, CTV-ΔCla M15, replicated at wild-type levels (Fig. 6C), suggesting the importance of the role of the SL1 secondary structure in replication.

The predicted SL1 structure also contained a single-stranded loop region at the terminus (nts 31 to 37; 5′-3′ AAAUACG). We constructed two mutants: CTV-ΔCla M16, in which the loop was deleted, and CTV-ΔCla M17, in which the nucleotides of the loop were substituted with nonviral nucleotides (5′-3′ GGCCUCA). The deletion of the loop sequence was predicted to shorten and change the pairing of nucleotides in the stem of SL1. The substitution of the loop sequences was predicted not to change the secondary structure of SL1 (Fig. 6B). Mutant CTV-ΔCla M16 failed to replicate, while CTV-ΔCla M17 replicated at reduced amounts compared to the wild-type construct (Fig. 6C). Overall, these data suggested that the predicted secondary structures of SL1 were essential for replication and that sequence alterations in the stems and the loop generally were tolerated with continued replication.

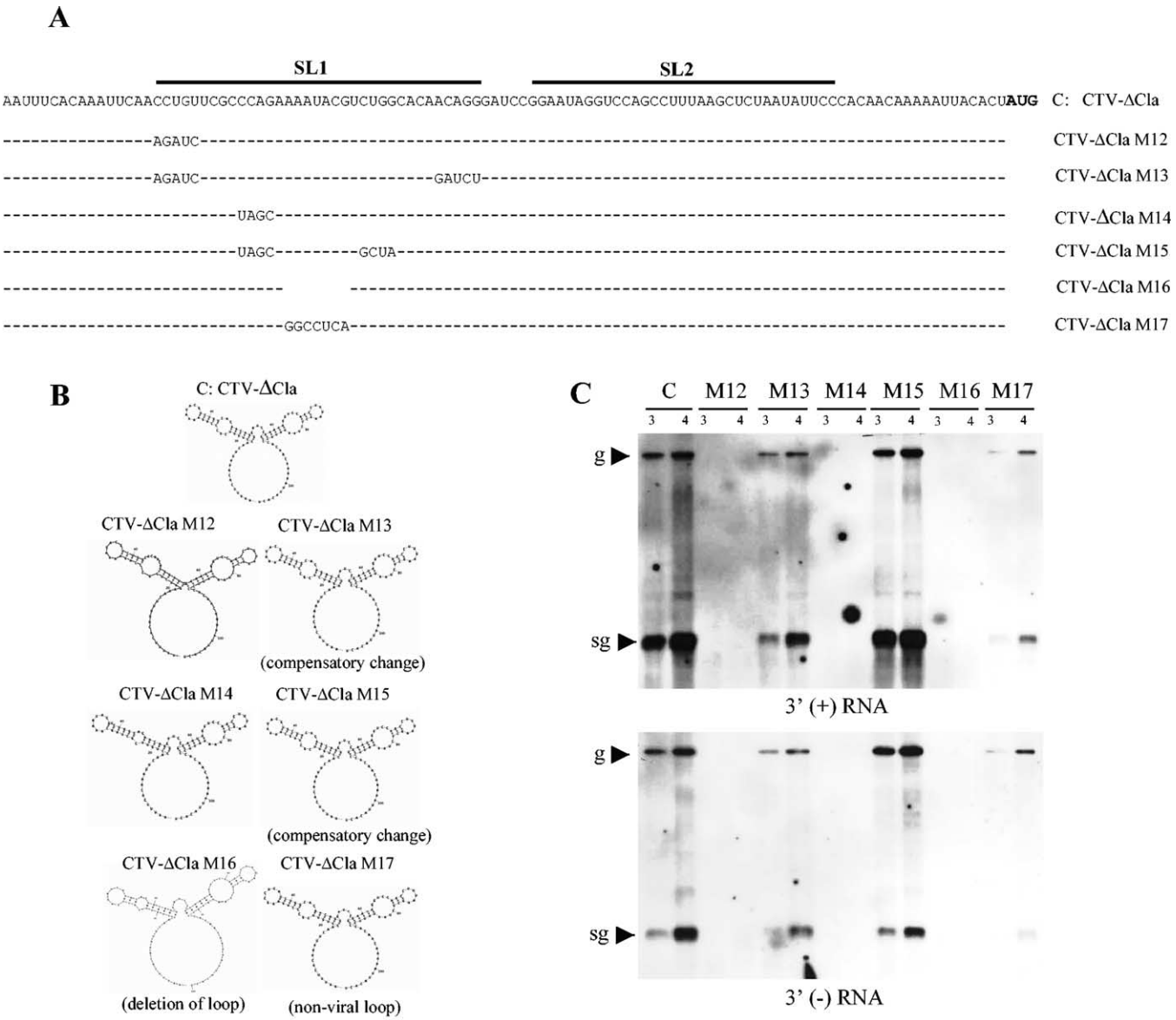

Fig. 6. (A) Schematic outline of the mutations in the SL1 region of 5′ NTR. The nucleotide sequence of the wild-type 5′ NTR (CTV-ΔCla) is presented and positions of the predicted SL1 and SL2 are outlined by thick black lines above the sequence. The nucleotide changes in the bottom-stem region (CTV-ΔClaM12) and the upper-stem region (CTV-ΔClaM14) and their respective compensatory changes (CTV-ΔClaM13 and CTV-ΔClaM15, respectively) are indicated. Deletion of the nucleotides of the upper loop (CTV-ΔClaM16) and substitution of the nucleotides of the loop with nonviral nucleotides (CTV-ΔClaM17) are also shown. (B) The predicted secondary structures of the positive-sense 5′ NTR of the wild-type replicon, CTV-ΔCla, and the mutants (CTV-ΔClaM12 to CTV-ΔClaM17) are shown. (C) Northern blot hybridization analysis of the total RNA isolated from the mesophyll protoplasts of *N. benthamiana* transfected with CTV-ΔCla and mutants CTV-ΔClaM12 to CTV-ΔClaM17. The blots were probed with positive-sense RNA-specific (top) or negative-sense RNA-specific (bottom) digoxigenin-labeled riboprobe. Positions of the genomic (g) and subgenomic (sg) RNAs are indicated by arrowheads.

Full-length CTV with mutations in the 5′ NTR sequences replicates but fails to be passaged in protoplasts

The mutations in the 5′ NTR that allowed near-wild-type levels of replication of CTV-ΔCla were examined in full-length CTV to ensure that the response of full-length CTV carrying the mutations in the 5′ NTR was similar to that of the CTV-ΔCla replicon containing the same mutation. To this end, we generated full-length CTV mutants CTV-9:M8, CTV-9:M9, CTV-9:M11, CTV-9:M13, and CTV-9:M15 with the same mutations in the 5′ NTR as those in the corresponding CTV-ΔCla mutants (Fig. 7A). CTV-9:M9, CTV-9:M11, and CTV-9:M15 replicated and produced genomic RNA and the full range of sgRNAs similar to that of the wild-type virus (CTV-9), while mutants CTV-9:M8 and CTV-9:M13 replicated at reduced levels compared to the wild-type virus (Fig. 7B).

Since the 5′ stem-loops appeared to be more conserved in the positive sequence, we examined whether the 5′ terminal mutations that allowed copious replication of the

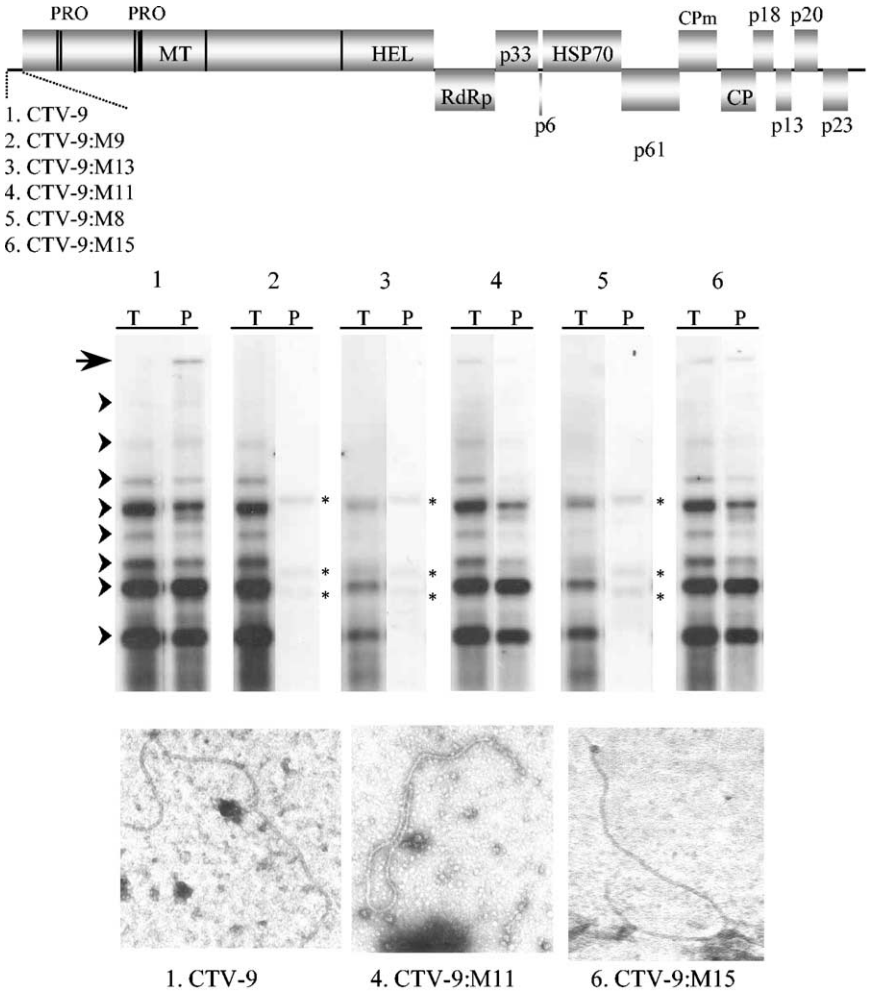

Fig. 7. Replication of the full-length CTV containing mutations in the 5′ NTR. A schematic representation of the full-length CTV (CTV9) containing 12 ORFs represented by open boxes, and two NTRs one at each end. The 5′ NTR mutations introduced into the full-length CTV are indicated (CTV9:M9, CTV9:M13, CTV9:M11, CTV9:M8, and CTV9:M15). Northern blot analysis of the total RNA isolated from *N. benthamiana* protoplasts 4 days posttransfection with the capped transcripts (T) and with the virions isolated from the transcript inoculated protoplasts (P). The blots were probed with the 3′ positive-strand specific digoxigenin-labeled riboprobe. The genomic and sgRNA positions are represented by an arrow and arrowheads, respectively. The asterisks indicate bands due to nonspecific hybridizations. Virions from protoplasts transfected with transcripts of CTV-9, and CTV-9:M11 and CTV-9:M15, trapped using CP polyclonal antiserum are shown at the lower part of the figure.

full-length virus would allow efficient assembly of virions. However, since in vitro produced RNA transcripts from full-length CTV infect only a minor proportion of protoplasts (on the order of 0.01 to 0.1%) resulting in a low level of progeny virions (Satyanarayana et al., 2001), a sensitive assay system was needed. We previously developed two effective methods to examine virions from this system. The first method is to view virus particles by serologically specific electron microscopy (SSEM), which allows concentration and visualization of partial and complete particles. Long virus particles that appeared to be full-length virions were seen in extracts of protoplasts transfected with mutants CTV-9:M11 or CTV-9:M15 (bottom of Fig. 7), but no virions were detected from extracts from protoplasts infected with mutants CTV-9:M9, CTV-9:M13, or CTV-9:M8, even though they produced relatively large amounts of genomic and sgRNAs in these protoplasts.

A more critical measure of stable and infectious virion particles is by the passage of virions in crude sap from transfected protoplasts to another set of protoplasts under conditions in which only complete particles have been shown to be passaged. Free RNA or partially encapsidated particles are approximately 10,000–100,000 less infectious than virions to inoculated protoplasts (Satyanarayana et al., 2001) and fail to be passaged under these conditions (Satyanarayana et al., 2000). The crude sap from the protoplasts transfected with CTV-9:M9, CTV-9:M13, and CTV-9:M8 almost totally failed to be passaged to the next batch of protoplasts, whereas progeny virions of CTV-9:M11 and CTV-9:M15 were passaged efficiently, similar to that of the wild-type virus (Fig. 7B).

These results demonstrate that the mutations of CTV-9:M9, CTV-9:M13, and CTV-9:M8 affected assembly of virions more than it affected the replication of RNA. Thus the

deletion of the upper stem and loop of SL2, and the altered sequences of the hinge area and the lower stem of SL1, inhibited virion assembly. Yet sequence changes in the lower stem of SL2 and the upper stem of SL1 did not affect production of infectious nucleocapsids.

Discussion

The first prediction of a common secondary structure for the 5′ NTR of CTV isolates resulted from analysis of sequences of 10 isolates representing three different sequence groups (López et al., 1998). Since that time other sequences from additional isolates (Ayllón et al., 2001) confirmed the original observation. Although a wide range of sequence variability was observed (intragroup sequence identity higher than 88% and intergroup sequence identity as low as 44%), the predicted structures of the positive-sense sequences were remarkably similar, especially the predicted SL1 and SL2. Yet, predicted secondary structures of the negative-sense sequences were variable.

Mutagenesis experiments supported the function of the predicted secondary structures of SL1 and SL2. Mutations that were predicted to alter the stem structures were lethal to replication, while compensatory mutations designed to rebuild the stem structures with different sequences allowed replication to resume at approximately wild-type levels. Overall, these data suggest that the predicted structures of SL1 and SL2 exist and are required for replication of CTV. Remarkably, alteration of the primary structure (compensatory mutations) of either stem or loop (heterologous loop) resulted in continued replication, suggesting little specificity for primary structure. Previously we examined the interaction of CTV replicase with heterologous *cis*-acting elements at the termini of the RNA by substituting heterologous terminal sequences from other strains into the CTV-ΔCla replicon (Satyanarayana et al., 1999). Sequences from other strains that are predicted to fold into similar secondary structures replicated, but at reduced levels. In general, the degree of continued replication was directly related to similarity to the homologous sequence, with termini containing more divergent sequences resulting in reduced replication. This demonstrated either a greater degree of specificity for primary structure or a more precise requirement for secondary structure than was obvious from our mutagenesis study.

Since the secondary structures of the CTV 5′ NTR were required for replication, which is thought to involve the sequential or joint interactions of the replicase complex with *cis*-acting elements from both 5′ and 3′ termini, it is tempting to speculate the conservation of at least some common structural features at both ends of the genome that interact with the replicase. We previously analyzed the structure-function relationship of the 3′ NTR (Satyanarayana et al., 2002). Yet, we do not recognize any readily discernible conserved sequences common to both termini.

The *cis*-acting elements in the 5′ NTR that are involved in replication have been characterized for many plus-stranded RNA viruses (cucumoviruses, tobraviruses, tymoviruses, tobamoviruses, and tobacco necrosis satellite virus). The BMV 5′ NTR sequences contain internal control region-like motifs that resemble the ICR 1 and ICR 2 of tRNA promoters (Marsh and Hall, 1987) necessary for replication (Pogue and Hall, 1992; Pogue et al., 1990, 1992). In *Alfalfa mosaic virus* (AMV) RNA 3, ICR-like motifs located in the 27-nt repeats of the 5′ NTR are required for virus replication (van der Vossen and Bol, 1996). The presence of ICR-like motifs in the 5′ NTR and the reduction of replication with mutated ICR-like motifs in BMV and AMV support the notion that host proteins probably bind to these structures, and the ability of this interaction determined initiation of plus-strand synthesis (Duggal and Hall, 1995; van der Vossen and Bol, 1996). Conserved structural elements and multiple sequences in the 5′ NTR of *Potato virus X* (PVX) were also observed to affect the accumulation of genomic and sgRNA (Miller et al., 1998; Kim and Hemenway, 1996). Recent studies in PVX have suggested the binding of a 54-kDa cellular protein, to nts 1–46 at the 5′ NTR (Kim et al., 2002).

Several observations and results suggest that the 5′ structural elements of CTV 5′ NTR required for replication function in the positive strand. First, the predicted structural elements are more conserved in the positive-strand among the different CTV isolates. Considerable variation occurs in predictions of minus-stranded structures. Second, the compensatory mutations that allowed resumption of wild-type levels of replication were not predicted to rebuild conserved negative-sense structures. Functional roles of plus-strand structures of the 5′ NTR in replication has been observed with viruses of other groups. The 5′ terminus of *Poliovirus* folded into cloverleaf structures in both positive and negative orientations, but only the positive-strand structure was functional (Andino et al., 1990). In BMV disruption of the positive-stranded RNA structure reduced the helper RNA-dependent replication of the pRNA in contrast to the disruption of the 3′ end of the negative-stranded stem-loop (Pogue and Hall, 1992). Similarly, it was shown that alterations of the secondary structure in the positive-strand of the 5′ NTR of a defective RNA of *Tomato bushy stunt virus* significantly decreased its ability to be replicated (Wu et al., 2001). In *Beet necrotic yellow vein virus*, a furovirus, mutations in the long 5′ NTR of RNA 3 that preferentially disrupted the interactions of Box II–II′ in the plus-strand structure replicated less efficiently compared to disruptions in Box II–II′ interactions in the minus-strand structure (Gilmer et al., 1993).

Previously, we found that the last 11 nts of the 3′ end of CTV could be deleted with reduced but continued replication (Satyanarayana et al., 2002). That result was unusual. Here, we found that 9 nts of the 5′ terminus also could be

Table 1
Synthetic oligonucleotides used and the mutants generated

Oligonucleotide	Sequence	Mutant generated
	nt 10 ↓	
C-370	5′-CACTCTCGAG**ATTTAGGTGACACTATAG**AATTCAACCTGTTCGCCCA	CTV-ΔCla M1
	nt 15 ↓	
C-390	5′-CAGTCTCGAG**ATTTAGGTGACACTATAG**AACCTGTTCGCCCAGAAAATAC	CTV-ΔCla M2
C-441	5′-CAGT**ATTTAGGTGACACTATAG**AATTTCACA*TGCAT*AACCTGTTCGCCAGAAA	CTV-ΔCla M3
	nt 97 nt 108 ↘ ↙	
C-443	5′-CTCTAATATTCCCACAACAAATGTCGAAACTCAGAGGAAG	CTV-ΔCla M4
	nt 93 nt 108 ↘ ↙	
C-496	5′-TTAAGCTCTAATATTCCCACATGTCGAAACTCAGAGGAAG	CTV-ΔCla M5
C-498	5′-AATACGTCTGGCACAACAGGGGAATAGGTCCAGCCTTTAA	CTV-ΔCla M6
C-518	5′-ACGTCTGGCACAACAGG*AGCAT*GGAATAGGTCCAGCCT	CTV-ΔCla M7
C-520	5′-TCTGGCACAACAGGGA*CATCGAT*TCCGAATAGGTCCAGC	CTV-ΔCla M8
	nt 68 nt 79 ↘ ↙	
C-406	5′-GATCCGGAATAGGTCCATCTAATATTCCCACAA	CTV-ΔCla M9
C-445	5′-GGCACAACAGGGATCC*TATTCC*GGTCCAGCCTTTAAGCT	CTV-ΔCla M10
C-508	5′-CAGCCTTTAAGCTCTAA*GGAATA*CACAACAAAATTAC	CTV-ΔCla M11
C-391	5′-CAGT**ATTTAGGTGACACTATAG**AATTTCACAAATTCAA*AGATC*TCGCCCAGAAAATACGTC	CTV-ΔCla M12
C-463	5′-AAATACGTCTGGCACA*GATCT*GATCCGGAATAGGTC	CTV-ΔCla M13
C-388	5′-CAG**TATTTAGGTGACACTATAG**AATTTCACAAATTCAACCTGTTCGC*TAGC*AAAATACGT CTGGCACAACAG	CTV-ΔCla M14
C-571	5′-TGTTCGC*TAGC*AAAATACGT*GCTA*CACAACAGGGATCCGGAATA	CTV-ΔCla M15
	nt 30 nt 38 ↘ ↙	
C-418	5′-TTCAACCTGTTCGCCCAGATCTGGCACAACAGGGATCC	CTV-ΔCla M16
C-420	5′—CAACCTGTTCGCCCAGA*GGCCTTA*TCTGGCACAACAGGGAT	CTV-ΔCla M17
C-171	5′-CCGTACCACACAGGACCG	

Note. Nucleotides in bold represent SP6 RNA polymerase promoter sequence incorporated into the oligonucleotide. Sequences of only the plus-sense oligonucleotides are shown except C-171. The minus-sense oligonucleotide, C-171 (nts 1164 to 1147), was used in the DNA amplification reaction with plus-sense primers, C-370, C-390, C-441, C-391, and C-388. Corresponding minus-sense sequences of the remaining plus-sense oligonucleotides were used in DNA amplification by overlap PCR. Sequences underlined and in italics indicated the mutated nucleotides. The numbers on the top of the oligonucleotide sequences, C-370 and C-390, represent the start of the CTV-specific sequences and the junction nucleotides in C-418, C-406, C-496, and C-443.

deleted with continued replication at wild-type levels. However, with this deletion the terminal nucleotides are in the same context as with the wild-type construct. Precise 5′ end nucleotides was a requirement for the efficient plus-stranded RNA synthesis in other viruses (Herold and Andino, 2000). It has been demonstrated that the tRNA-like structure of BMV and other viruses function as a telomere for protection of the 3′ terminus. Perhaps CTV has flexible termini as a mechanism to stabilize the RNA.

In vitro assembly experiments with the potexvirus, *Papaya mosaic virus*, have identified 38–47 nts at the 5′ terminus required for initiation of virion assembly (Abouhaidar and Bancroft, 1978; Sit et al., 1994). In *Turnip yellow mosaic virus*, a tymovirus, the 5′ NTR is involved in both replication and assembly (Hellendoorn et al., 1997). Encapsidation efficiency of the virus was severely affected in mutants lacking the protonatable mismatches in internal loops of two predicted conserved stem loops, suggesting binding of the coat protein to the protonated cytosines in the 5′ proximal hairpin (Bink et al., 2002) and recently it was shown that the stability of the 5′ proximal hairpin of the 5′ NTR regulated translation efficiency and initiation of encapsidation (Bink et al., 2003). Double-hairpin structures in the 5′ NTR (SL1 and SL3) of human immunodeficiency virus type 1 also have been shown to contribute to virion formation (McBride and Panganiban, 1997).

CTV virion assembly is probably more complex compared to other viral systems of plants. The efficient assembly requires four gene products: two coat proteins (CP and CPm), an HSP70h, and p61 (Satyanarayana et al., 2000), although low level of assembly was observed with only CP or CPm (Satyanarayana et al., unpublished data). The homologs of HSP70h and p61 have been found associated with virions in other members of the *Closteroviridae* (Tian et al., 1999; Napuli et al., 2000) and have been suggested to be involved in virion assembly (Alzanova et al., 2001; Napuli et al., 2003). However, it is not clear if these proteins

are minor structural components necessary to the virion architecture or contaminants after functioning in the assembly process. The two CPs encapsidate opposite ends of the virion RNA with a transition approximately 5% from one end (Febres et al., 1996). It is possible that each coat protein has a different origin of assembly. The data presented here suggest that the primary structure (sequence) of a subset of this region is necessary for assembly. Perhaps this component is an assembly origin for one of the two CPs of CTV.

Materials and methods

Construction of plasmids

Infectious cDNA clone of CTV (CTV9), CTV replicon (CTV-ΔCla), and a modified CTV-ΔCla that contained a unique *Stu*I restriction site at the 5′ end of the SP6 RNA polymerase promoter engineered upstream of 5′ NTR sequence (Satyanarayana et al. 1999) were used as the parent plasmids to generate the mutants used in this study. The nucleotide sequence and numbering of the oligonucleotide primers used in this study were according to Satyanarayana et al. (2003) (Accession No. AY170468). The mutations were generated in the 5′ NTR by overlap extension PCR technique (Ho et al., 1989) using a pair of plus- and minus-sense oligonucleotides that contained desired mutations (Table 1). The outer 5′ primer contained the SP6 polymerase promoter sequence, while the 3′ minus primer (nts 1147–1164) contained CTV-specific sequence 3′ of the unique *Bgl*II restriction site (nt 1029) in CTV-ΔCla. Overlap extension amplification products were digested with *Bgl*II and ligated between *Stu*I- and *Bgl*II-digested CTV-)Cla.

Selected mutants that contained mutations in the 5′ NTR of CTV-ΔCla (CTV-ΔCla M8, CTV-ΔCla M9, CTV-ΔCla M11, CTV-ΔCla M 13, and CTV-ΔCla M15) were transferred into the full-length CTV by exchanging the unique *Nco*I and *Not*I restriction enzyme digested product from CTV9 and ligated into similarly digested 5′ NTR mutants to generate CTV-9:M8, CTV-9:M9, CTV-9:M11, CTV-9:M13, and CTV-9:M15, respectively. All the mutants were sequenced for the presence of the desired mutation in the 5′ NTR.

Comparison of the 5′ NTR sequences from different isolates [T36, NC_001661; T30, AF260651; VT, U56902; T385, Y18420; SY568, AF001623; NUagA, AB046398, and T68 (M. Hilf, Personal Communication)] was carried out using CLUSTAL program (Thompson et al., 1994), and the putative most stable secondary structures were predicted using *MFOLD* program (Zuker et al., 1999).

Isolation and transfection of protoplasts, and analysis of viral RNA

Isolation of *N. benthamiana* mesophyll protoplasts, synthesis of SP6 RNA polymerase-dependent RNA transcripts from *Not*I linearized cDNAs, subsequent PEG-mediated transfection of protoplasts, and Northern blot analysis of the total RNA using digoxigenin-labeled strand-specific riboprobes were carried out as outlined earlier (Navas-Castillo et al., 1997; Satyanarayana et al., 1999).

Assay for virion assembly

Assembly of CTV virions was examined by SSEM in extracts of transfected protoplasts and by passage of virions in the crude sap from transfected protoplasts to a second batch of protoplasts as described earlier (Satyanarayana et al., 2000, 2001). Briefly, transcript inoculated protoplasts were harvested 4 dpi and gently suspended in 40 mM sodium phosphate buffer (pH 8.2) over period of 30 min. The suspension was clarified by low-speed centrifugation (4000 rpm) and the supernatant was used to inoculate a fresh batch of protoplasts using PEG as outlined by Satyanarayana et al. (2000).

Acknowledgments

The authors thank John Cook, Judy Harber, and Cecile Robertson for technical assistance; Dr. Moshe Bar-Joseph for critically reading the manuscript and Dianne Achor for help with electron microscope. This research was supported by an endowment from the J.R. and Addie Graves family, grants from the Florida Citrus Production Research Advisory Board, the Florida Agricultural Experiment Station, the U.S.–Israel BARD and USDA/ARS cooperative Agreement 58-6617-4-018 and was approved for publication as University of Florida Agricultural Experiment Station Journal Series Number R-09612.

References

Abouhaidar, M., Bancroft, J.B., 1978. The initiation of papaya mosaic virus assembly. Virology 90, 54–59.

Albiach-Marti, R., Mawassi, M., Gowda, S., Satyanarayana, T., Hilf, M.E., Shanker, S., Almira, E.C., Vives, M.C., López, C., Guerri, J., Flores, R., Moreno, P., Garnsey, S.M., Dawson, W.O., 2000. Sequences of Citrus tristeza virus separated in time and space are essentially identical. J. Virol. 74, 15–23.

Alzhanova, D.V., Napuli, A.J., Creamer, R., Dolja, V.V., 2001. Cell-to-cell movement and assembly of a plant closterovirus: roles for the capsid proteins and Hsp70 homolog. EMBO J. 17, 6997–7007.

Andino, A.H., Rieckhof, G.E., Baltimore, D., 1990. A functional ribonucleoprotein complex forms around the 5′ end of poliovirus RNA. Cell 63, 369–380.

Ayllón, M.A., López, C., Navas-Castillo, J., Garnsey, S.M., Guerri, J., Flores, R., Moreno, P., 2001. Polymorphism of the 5′ terminal region of citrus tristeza virus (CTV) RNA: incidence of three sequence types in isolates of different origin and pathogenicity. Arch. Virol. 146, 27–40.

Barton, D.J., O'Donnell, B.J., Flanegan, J.B., 2001. 5′ clover-leaf in poliovirus RNA is a cis-acting replication element required for negative-strand synthesis. EMBO J. 15, 1439–1448.

Bink, H.H.J., Hellendoorn, H.K., van der Meulen, J., Pleij, C.W.A., 2002. Protonation of non-Watson-Crick base pairs and encapsidation of turnip yellow mosaic virus. Proc. Natl. Acad. Sci. USA 99, 13465–13470.

Bink, H.H.J., Schirawski, J., Haenni, A-L., Pleij, C.W.A., 2003. The 5′-proximal hairpin of turnip yellow mosaic virus RNA: its role in translation and encapsidation. J. Virol. 77, 7452–7458.

Buck, K.W., 1996. Comparison of the replication of the positive-stranded RNA viruses of plants and animals. Adv. Virus Res. 47, 159–251.

Corver, J., Lenches, E., Smith, K., Robison, R.A., Sando, T., Strauss, E.G., Strauss, J.H., 2003. Fine mapping of a cis-acting sequence element in yellow fever virus RNA that is required for RNA replication and cyclization. J. Virol. 77, 2265–2270.

Dreher, T.W., 1999. Functions of the 3′-untranslated regions of positive strand RNA viral genomes. Annu. Rev. Phytopathol. 37, 151–174.

Duggal, R., Hall, T.C., 1995. Interaction of host proteins with the plus-strand promoter of brome mosaic virus RNA-2. Virology 214, 638–641.

Duggal, R., Lahser, F.C., Hall, T.C., 1994. Cis-acting sequences in the replication of plant viruses with plus-sense RNA genomes. Annu. Rev. Phytopathol. 32, 287–309.

Febres, V.J., Ashoulin, L., Mawassi, M., Frank, A., Bar-Joseph, M., Manjunath, K.L., Lee, R.F., Niblett, C.L., 1996. The p27 protein is present at one end of citrus tristeza virus particles. Phytopathology 86, 1331–1335.

Gilmer, D., Allmang, C., Ehresmann, C., Guilley, H., Richards, K., Jonard, G., Ehresmann, B., 1993. The secondary structure of the 5′-noncoding region of beet necrotic yellow vein virus RNA 3: evidence for a role in viral RNA replication. Nucleic Acids Res. 21, 1389–1395.

Guan, H., Song, C., Simon, A.E., 1997. RNA promoters located on (−)-strands of a subviral RNA associated with turnip crinkle virus. RNA 3, 1401–1412.

Hellendoorn, K., Verlaan, P.W.G., Pleij, C.W.A., 1997. A functional role for the conserved protonatable hairpins in the 5′ untranslated region of turnip yellow mosaic virus RNA. J. Virol. 71, 8774–8779.

Herold, J., Andino, R., 2000. Poliovirus requires precise 5′ end for efficient positive-strand RNA synthesis. J. Virol. 74, 6394–6400.

Hilf, M.E., Karasev, A.V., Pappu, H.R., Gumpf, D.J., Niblett, C.L., Garnsey, S.M., 1995. Characterization of citrus tristeza virus subgenomic RNAs in infected tissue. Virology 208, 576–582.

Ho, S.N., Hunt, H.D., Horton, R.M., Puller, J.K., Pease, L.R., 1989. Site-directed mutagenesis by overlap extension using polymerase chain reaction. Gene 77, 51–59.

Karasev, A.V., Boyko, V.P., Gowda, S., Nikolaeva, O.V., Hilf, M.E., Koonin, E.V., Niblett, C.L., Cline, K., Gumpf, D.J., Lee, R.F., Garnsey, S.M., Lewandowski, D.J., Dawson, W.O., 1995. Complete sequence of the citrus tristeza virus RNA genome. Virology 208, 511–520.

Kim, K-H., Hemenway, C.L., 1996. The 5′ nontranslated region of poato virus x RNA affects both genomic and subgenomic RNA synthesis. J. Virol. 70, 5533–5540.

Kim, K-H., Kwon, S-J., Hemenway, C.L., 2002. Cellular protein binds to sequences near the 5′ terminus of potato virus X RNA that are important for replication. Virology 301, 305–312.

López, C., Ayllón, M.A., Navas-Castillo, J., Guerri, J., Moreno, P., Flores, R., 1998. Molecular variability of the 5′- and 3′-terminal regions of citrus tristeza virus. Phytopathology 7, 685–691.

Marsh, L.E., Hall, T.C., 1987. Evidence implicating a tRNA heritage for the promoters of (+) strand RNA synthesis in brome mosaic virus and related viruses. Cold Spring Harbor Symp. Quant. Biol. 52, 331–341.

Mawassi, M., Mietkiewska, E., Goffman, R., Yang, G., Bar-Joseph, M., 1996. Unusual sequence relationships between two isolates of citrus tristeza virus. J. Gen. Virol. 77, 2359–2364.

McBride, S.M., Panganiban, A.T., 1997. Position dependence of functional hairpins important for human immunodeficiency virus type 1 RNA encapsidation in vivo. J. Virol. 71, 2050–2058.

Miller, E.D., Kim, K-H., Hemenway, C.L., 1999. Restoration of a stem-loop structure required for potato virus X RNA accumulation indicates selection for a mismatch and a GNRA tetraloop. Virology 260, 342–353.

Miller, E.D., Plante, C.A., Kim, K-H., Brown, J.W., Hemenway, C.L., 1998. Stem-loop structure in the 5′ region of Potato virus X genome required for plus-strand RNA accumulation. J. Mol. Biol. 284, 591–608.

Miller, W.A., Koev, G., 2000. Synthesis of subgenomic RNAs by positive strand RNA viruses. Virology 273, 1–8.

Nagy, P.D., Pogany, J., 2000. Partial purification and characterization of Cucumber necrosis virus and Tomato bushy stunt virus RNA-dependent RNA polymerases: similarities and differences in template usage between tobamovirus and carmovirus RNA-dependent RNA polymerases. Virology 276, 279–288.

Napuli, A.J., Alzhanova, D.V., Doneanu, C.E., Barofsky, D.F., Koonin, E.V., Dolja, V.V., 2003. The 64-kilodalton capsid protein homolog of Beet yellows virus is required for assembly of virion tails. J. Virol. 77, 2377–84.

Napuli, A.J., Falk, B.W., Dolja, V.V., 2000. Interaction between HSP70 homolog and filamentous virions of Beet yellows virus. Virology 274, 232–239.

Navas-Castillo, J., Albiach-Martí, M.R., Gowda, S., Hilf, M.E., Garnsey, S.M., Dawson, W.O., 1997. Kinetics of accumulation of citrus tristeza virus RNAs. Virology 228, 92–97.

Panavas, T., Nagy, P.D., 2003. The RNA replication enhancer element of tombusviruses contains two interchangeable hairpins that are functional during plus-strand synthesis. J. Virol. 77, 258–269.

Panavas, T., Panaviene, Z., Pogany, J., Nagy, P.D., 2003. Enhancement of RNA synthesis by promoter duplication in tombusviruses. Virology 310, 118–129.

Pappu, H.R., Karasev, A.V., Anderson, E.J., Pappu, S.S., Hilf, M.E., Febres, V.J., Eckloff, R.M.G., McCaffery, M., Boyko, V.P., Gowda, S., Dolja, V.V., Koonin, E.V., Gumpf, D.J., Cline, K.C., Garnsey, S.M., Dawson, W.O., Lee, R., Niblett, C.L., 1994. Nucleotide sequence and organization of eight 3′ open reading frames of the citrus tristeza closterovirus genome. Virology 199, 35–46.

Pogue, G.P., Hall, T.C., 1992. The requirement of a 5′ stem-loop structure in brome mosaic virus replication supports a new model for viral positive-strand RNA initiation. J. Virol. 66, 674–684.

Pogue, G.P., Marsh, L.E., Connel, J.P., Hall, T.C., 1992. Requirement of ICR-like sequences in the replication of brome mosaic virus genomic RNA. Virology 188, 742–753.

Pogue, G.P., Marsh, L.E., Hall, T.C., 1990. Point mutations in the ICR2 motif of brome mosaic virus RNAs debilitate (+)-strand replication. Virology 178, 152–160.

Satyanarayana, T., Bar-Joseph, M., Mawassi, M., Albiach-Martí, M.R., Ayllón, M.A., Gowda, S., Hilf, M.E., Moreno, P., Garnsey, S.M., Dawson, W.O., 2001. Amplification of citrus tristeza virus from a cDNA clone and infection of citrus trees. Virology 280, 87–96.

Satyanarayana, T., Gowda, S., Ayllón, M.A., Albiach-Martí, M.R., Dawson, W.O., 2002. Mutational analysis of the replication signals in the 3′-nontranslated region of Citrus tristeza virus. Virology 300, 140–152.

Satyanarayana, T., Gowda, S., Ayllón, M.A., Dawson, W.O., 2003. Frameshift mutations in infectious cDNA clones of *Citrus tristeza virus:* a strategy to minimize toxicity of viral sequences to *Escherichia coli*. Virology 313, 481–491.

Satyanarayana, T., Gowda, S., Boyko, V.P., Albiach-Martí, M.R., Mawassi, M., Navas-Castillo, J., Karasēv, A.V., Dolja, V.V., Hilf, M.E., Lewandowski, D.J., Moreno, P., Bar-Joseph, M., Garnsey, S.M., Dawson, W.O., 1999. An engineered closterovirus RNA replicon and analysis of heterologous terminal sequences for replication. Proc. Natl. Acad. Sci. USA 96, 7433–7438.

Satyanarayana, T., Gowda, S., Mawassi, M., Albiach-Martí, M.R., Ayllón, M.A., Robertson, C.R., Garnsey, S.M., Dawson, W.O., 2000. Closterovirus encoded HSP70 homolog and p61 in addition to both coat proteins function in efficient virion assembly. Virology 278, 253–265.

Sit, T.L., Leclerc, D., Abouhaidar, M., 1994. The minimal 5′ sequence for in vitro initiation of papaya mosaic virus potexvirus assembly. Virology 199, 238–242.

Sivakumaran, K., Kao, C.C., 1999. Initiation of genomic plus-strand RNA synthesis from DNA and RNA templates by a viral RNA-dependent RNA polymerase. J. Virol. 73, 6415–6423.

Thompson, J.D., Higgins, D.G., Gibson, T.J., 1994. CLUSTAL W: improving the sensitivity of progressive multiple sequence alignment through sequence weighting, position-specific gap penalties and weight matrix choice. Nucleic Acids Res. 22, 4673–4680.

Tian, T., Rubio, L., Yeh, H.-H., Crawford, B., Falk, B.W., 1999. Lettuce infectious yellows virus: in vitro acquisition analysis using partially purified virions and the whitefuly, *Bemisia tabaci*. J. Gen. Virol. 80, 1111–1117.

Turner, R.L., Buck, K.W., 1999. Mutational analysis of cis-acting sequences in the 3′- and 5′-untranslated regions of red clover necrotic mosaic virus. Virology 253, 115–124.

van der Vossen, E.A.G., Bol, J.F., 1996. Analysis of cis-acting elements in the 5′ leader sequence of alfalfa mosaic virus RNA3. Virology 220, 539–543.

Wu, B., Vanti, W.B., White, K.A., 2001. An RNA domain within the 5′ untranslated region of the Tomato bushy stunt virus genome modulated viral RNA replication. J. Mol. Biol. 305, 741–756.

Zuker, M., Mathews, D.H., Turner, D.H., 1999. Algorithms and thermodynamics for RNA secondary structure prediction. A practical guide, in: Barciszewski, J., Clark, B.F.C. (Eds.), RNA Biochemistry and Bio/Technology, Kluwer Academic Publishers, Dordrecht/Norwell, MA, pp. 11–43.